Influence of initial mean helicity on homogeneous turbulent shear flow

Frank G. Jacobitz,[1,2,*] Kai Schneider,[2,†] Wouter J. T. Bos,[3,‡] and Marie Farge[4,§]

[1]*Mechanical Engineering Program, University of San Diego, 5998 Alcalá Park, San Diego, CA 92110, USA*
[2]*M2P2–CNRS & CMI, Université de Provence, 39, rue Joliot-Curie, 13453 Marseille Cedex 13, France*
[3]*LMFA–CNRS, Ecole Centrale de Lyon, Université de Lyon, 36, avenue Guy-de-Collongue, 69134 Ecully Cedex, France*
[4]*LMD–CNRS, Ecole Normale Supérieure, 24, rue Lhomond, 75231 Paris Cedex 5, France*

Helicity statistics are studied in homogeneous turbulent shear flow. Initial mean helicity is imposed on an isotropic turbulence field using a decomposition of the flow into complex-valued helical waves. The initial decay of the turbulent kinetic energy is weakened in the presence of strong mean helicity, consistent with an analytic analysis of the spectral tensor of velocity correlations. While exponential growth of the mean turbulent kinetic energy is obtained, the mean helicity decays. Probability distribution functions (PDFs) of helicity are skewed and show that the imposed mean helicity prevails throughout the simulations. A wavelet-based scale-dependent analysis shows a trend to two dimensionalization for large scales of motion and a preference for helical motion at small scales. The magnitude of the skewness of the PDFs decreases for smaller scales. Joint PDFs indicate a strong correlation of the signs of both, helicity and superhelicity, for all cases. This correlation supports the conjecture that superhelicity dissipates helicity.

I. INTRODUCTION

Helicity $H_u = \boldsymbol{u} \cdot \boldsymbol{\omega}$ is defined as the scalar product of velocity $\boldsymbol{u}$ and vorticity $\boldsymbol{\omega} = \nabla \times \boldsymbol{u}$ and relative helicity $h_u = H_u/(|\boldsymbol{u}||\boldsymbol{\omega}|)$ is thus the cosine of the angle between the two vectors. It allows us to distinguish between helical and nonhelical structures. Helical structures or swirling motion are characterized by $h_u = \pm 1$, which correspond to alignment or anti-alignment of velocity and vorticity, respectively. Nonhelical structures or two dimensionalization of a flow are characterized by $h_u = 0$, implying that velocity is perpendicular to vorticity.

Helicity is observed in atmospheric flows and, for example, it plays an important role in the formation and evolution of tornadoes [1]. Helicity is also essential in magnetohydrodynamics of conducting fluids, in particular for the dynamo effect [2]. It further plays a crucial role in the problem of relaxation toward magnetostatic equilibrium, a problem of central importance in the context of magnetically confined thermonuclear fusion plasma [1]. Historically, helicity was first introduced by Betchov [3], Moreau [4], and Moffatt [5]. A comprehensive review on helicity can be found in Moffatt and Tsinober [1].

Energy and helicity are inviscid quadratic invariants of three-dimensional isotropic turbulence. While energy and enstrophy cascade in opposite directions in two-dimensional turbulence, there is evidence that energy and helicity have a joint cascade in three-dimensional turbulence [6–8]. The dynamical importance of helicity is associated to its role in the reduction of energy transfer. Kraichnan [8] predicted, by consideration of the interaction between pure helical waves, that energy transfer would be slowed down by helical motion,

since waves with opposite helicity interact more strongly than waves with the same helicity. This tendency to slow down the transfer was first observed in a two-point closure study by André and Lesieur [9], in which the initial energy decay was reduced in the presence of helicity.

The fact that helicity leads to the reduction of nonlinear transfer can also be inferred from the fact that, in the case of maximum helicity, vorticity is parallel or antiparallel to velocity and therefore the Lamb vector $\boldsymbol{\ell} = \boldsymbol{u} \times \boldsymbol{\omega}$ vanishes. Since the nonlinear term in the Navier-Stokes equations is equal to the solenoidal part of the Lamb vector, the case of maximum helicity is unfavorable for nonlinear interaction. In this context it was suggested [10,11] that local helicity fluctuations play an important role in the reduction of nonlinear interaction observed in turbulent flows. However, Kraichnan and Panda [12] showed that local helicity fluctuations are not enough to explain the observed reduction of nonlinearity, but that a certain preferential alignment of the wave vector and the Lamb vector is needed to explain the observed reduction of nonlinear interaction. Even though this study showed that local helicity fluctuations might not be the sole actor in the reduction of nonlinear transfer, helicity, at least in the average sense, plays a role in it [13].

Apart from its dynamical significance, helicity is also an important topological quantity to characterize turbulence. Helicity allows a topological interpretation of the linkages of vortex lines present in the flow. Vortex sheets are nonhelical and therefore necessarily separated from regions of maximal helicity. This has led to the speculation that there should be an anticorrelation between helicity and energy dissipation [1]. The helical properties of isotropic turbulence, in particular the inertial range scaling and the interscale flux of energy and helicity, have been examined in the past by direct numerical simulations [6,7]. High-resolution direct numerical simulations of forced helical rotating turbulence have been performed more recently to investigate integral quantities and their spectral distribution [14] as well as their intermittency

*jacobitz@sandiego.edu
†kschneid@cmi.univ-mrs.fr
‡wouter.bos@ec-lyon.fr
§farge@lmd.ens.fr

properties [15]. Helicity and its transfer have also been studied in the context of shell models of isotropic turbulence in Benzi *et al.* [16] and Biferale *et al.* [17]. To our knowledge, however, the influence of initial helicity on homogeneous shear flow has not been studied.

In this work the helicity statistics in growing homogeneous turbulent shear flow are investigated. The goals of this study are an investigation of the impact of initial mean helicity on the evolution of the turbulent kinetic energy, the statistical properties of helicity at various scales of the turbulent motion following the wavelet-based scale-dependent analysis of Ref. [18], and an investigation on the role of the superhelicity, defined as the scalar product of vorticity with its curl, in the dissipation of helicity.

II. GOVERNING EQUATIONS

Homogeneous turbulence subjected to a uniform mean velocity gradient is considered. The mean gradient is chosen, without loss of generality, as

$$\sigma_{ij} = \frac{\partial \langle U_i \rangle}{\partial x_j} = S\delta_{i1}\delta_{j2}. \tag{1}$$

The total velocity U can then be decomposed into mean $\langle U \rangle = Sx_2 e_1$ (as shown in Fig. 1) and fluctuations u. The governing equations for the fluctuating quantities are

$$\nabla \cdot u = 0, \tag{2}$$

$$\frac{\partial u}{\partial t} + u \cdot \nabla u + Sx_2 \frac{\partial u}{\partial x_1} + Su_2 e_1 = -\frac{1}{\rho_0}\nabla p + \nu\nabla^2 u. \tag{3}$$

Here S is the shear rate of the mean velocity, p is the pressure, ρ_0 is the density, ν is the kinematic viscosity of the fluid, and e_1 is the unit vector in the x_1 direction. The evolution of the turbulent kinetic energy $K = \langle u \cdot u \rangle/2$ is given by

$$\frac{dK}{dt} = -S\langle u_1 u_2 \rangle - 2\nu Z, \tag{4}$$

where $Z = \langle \omega \cdot \omega \rangle/2$ is the enstrophy. Similar to energy, the mean helicity $\langle H_u \rangle = \int H_u d^3x$ satisfies a balance equation

$$\frac{d}{dt}\langle H_u \rangle = \langle F \rangle - 2\nu\langle H_\omega \rangle, \tag{5}$$

where $H_\omega = \omega \cdot (\nabla \times \omega)$ is the superhelicity and $F = 2f \cdot \omega$ accounts for forcing terms f in the momentum equation (3). Contrary to energy, neither helicity H_u nor superhelicity H_ω are positive definite quantities. Therefore, the term involving superhelicity in Eq. (5) can only be interpreted as a helicity dissipation term if $\langle H_u \rangle$ and $\langle H_\omega \rangle$ have the same sign. Considering isotropic turbulence, Sanada [19] conjectured that $\langle H_u \rangle$ and $\langle H_\omega \rangle$ indeed have the same sign and thus the superhelicity term acts as a dissipative mechanism for helicity. Further evidence supporting Sanada's conjecture was more recently given by Galanti and Tsinober [20] for isotropic turbulence with helical or nonhelical forcing.

Note that the forcing term $\langle F \rangle$ in Eq. (5) vanishes if the flow possesses a mirror symmetry property. This is also the case in the current flow geometry. In such flows, mean helicity can only be studied in two ways: First, an artificial helical forcing is applied to the simulations. This approach was used by a variety of previous studies of homogeneous isotropic
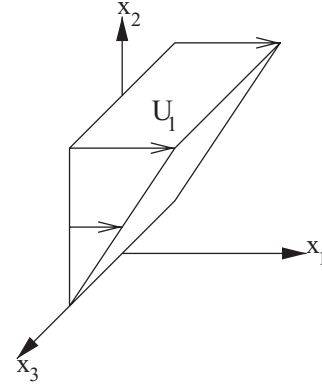

FIG. 1. Schematic of the flow.

turbulence [6,20]. Second, mean helicity is introduced into the initial conditions and it is then allowed to decay throughout the simulations. Morinishi *et al.* [21] proposed an approach to introduce helicity into a turbulent flow, based on the helical wave decomposition. They then studied the impact of initial mean helicity on decaying rotating homogeneous turbulence. It was shown that helicity and rotation inhibit the energy transfer through different mechanisms: helicity diminishes nonlinear interactions globally, whereas rotation concentrates nonlinear interactions to resonant triads of inertial waves.

Since we are interested in the influence of helicity on the evolution of the flow, the equation for the spectral tensor, defined as the Fourier transform of the double correlation of velocity at two points, is considered. The energy evolution involves an intricate interaction of the turbulence with the mean shear, resulting in turbulence production, and transfer between scales through nonlinear mode couplings, eventually resulting in turbulence dissipation. Spectral or other multiscale techniques are required in order to analyze the underlying mechanisms. The spectral tensor is defined by

$$\Phi_{ij}(\boldsymbol{k})\delta(\boldsymbol{k} + \boldsymbol{p}) = \langle \widehat{u}_i(\boldsymbol{k})\widehat{u}_j(\boldsymbol{p}) \rangle, \tag{6}$$

where $\widehat{u}_i(\boldsymbol{k})$ is the Fourier transform of the velocity and $\boldsymbol{k}$ the wave vector. The evolution equation of this quantity for the case of homogeneous shear flow can be found for example in Cambon *et al.* [22]:

$$\left(\frac{\partial}{\partial t} + 2\nu k^2\right)\Phi_{ij}(\boldsymbol{k})$$

$$= -\sigma_{il}\Phi_{lj}(\boldsymbol{k}) - \sigma_{jl}\Phi_{il}(\boldsymbol{k}) + \sigma_{ln}k_l\frac{\partial \Phi_{ij}(\boldsymbol{k})}{\partial k_n}$$

$$+ 2\sigma_{ln}\left[\frac{k_l k_i}{k^2}\Phi_{nj}(\boldsymbol{k}) + \frac{k_l k_j}{k^2}\Phi_{in}(\boldsymbol{k})\right] + \Omega_{ij}(\boldsymbol{k}). \tag{7}$$

In this expression the last term $\Omega_{ij}(\boldsymbol{k})$ corresponds to the unclosed triple correlation terms, leading to nonlinear transfer. In order to investigate the effects of helicity, we decompose the spectral tensor into its mirror symmetric term $\phi_{ij}(\boldsymbol{k})$ and its helical contribution $\mathcal{H}_{ij}(\boldsymbol{k})$:

$$\phi_{ij}(\boldsymbol{k}) = \tfrac{1}{2}[\Phi_{ij}(\boldsymbol{k}) + \Phi_{ji}(\boldsymbol{k})], \tag{8}$$

$$\mathcal{H}_{ij}(\boldsymbol{k}) = \tfrac{1}{2}[\Phi_{ij}(\boldsymbol{k}) - \Phi_{ji}(\boldsymbol{k})]. \tag{9}$$

Combining (7) and (8) we find for the evolution of ϕ_{ij}:

$$\left(\frac{\partial}{\partial t} + 2\nu k^2\right)\phi_{ij}(\boldsymbol{k})$$

$$= -\sigma_{il}\phi_{lj}(\boldsymbol{k}) - \sigma_{jl}\phi_{il}(\boldsymbol{k}) + \sigma_{ln}k_l\frac{\partial\phi_{ij}(\boldsymbol{k})}{\partial k_n}$$

$$+ 2\sigma_{ln}\left[\frac{k_lk_i}{k^2}\phi_{nj}(\boldsymbol{k}) + \frac{k_lk_j}{k^2}\phi_{in}(\boldsymbol{k})\right]$$

$$+ \frac{1}{2}[\Omega_{ij}(\boldsymbol{k}) + \Omega_{ji}(\boldsymbol{k})]. \qquad (10)$$

The equation for the helical contribution is similarly obtained and reads

$$\left(\frac{\partial}{\partial t} + 2\nu k^2\right)\mathcal{H}_{ij}(\boldsymbol{k})$$

$$= -\sigma_{il}\mathcal{H}_{lj}(\boldsymbol{k}) - \sigma_{jl}\mathcal{H}_{il}(\boldsymbol{k}) + \sigma_{ln}k_l\frac{\partial\mathcal{H}_{ij}(\boldsymbol{k})}{\partial k_n}$$

$$+ 2\sigma_{ln}\left[\frac{k_lk_i}{k^2}\mathcal{H}_{nj}(\boldsymbol{k}) + \frac{k_lk_j}{k^2}\mathcal{H}_{in}(\boldsymbol{k})\right]$$

$$+ \frac{1}{2}[\Omega_{ij}(\boldsymbol{k}) - \Omega_{ji}(\boldsymbol{k})]. \qquad (11)$$

Using once more the symmetry property of the helical part, this last equation simplifies to

$$\left(\frac{\partial}{\partial t} + 2\nu k^2\right)\mathcal{H}_{ij}(\boldsymbol{k})$$

$$= \sigma_{ln}k_l\frac{\partial\mathcal{H}_{ij}(\boldsymbol{k})}{\partial k_n} + \frac{1}{2}[\Omega_{ij}(\boldsymbol{k}) - \Omega_{ji}(\boldsymbol{k})]. \qquad (12)$$

From Eqs. (10) and (12) it follows that the interaction of the mirror symmetric and helical parts of the spectral tensor are only coupled through nonlinear interactions, represented by Ω_{ij}. Shear does appear in Eq. (12) in the linear transfer term, which corresponds to a redistribution of the helicity in Fourier space, but does not produce any helicity. The linear interactions of the shear with the mirror symmetric part of the turbulent fluctuations do not involve the helical part and vice versa. In other words, $\mathcal{H}_{ij}(\boldsymbol{k})$ does not explicitly appear in Eq. (10) and $\phi_{ij}(\boldsymbol{k})$ does not appear in Eq. (12). Since the kinetic energy is given by the mirror symmetric part $[K = (1/2)\int\phi_{ii}(\boldsymbol{k})d\boldsymbol{k}]$, helicity influences the evolution of energy only through the nonlinear interaction. In order to better understand this nonlinear coupling between the helical and the nonhelical part of the

turbulence, one needs a closure assumption for Ω_{ij} or one can directly simulate the Navier-Stokes equations. It is this second approach that will be adopted in the present investigation.

III. SIMULATION APPROACH

The direct numerical simulations performed here are based on the continuity equation (2) for an incompressible fluid and the unsteady three-dimensional Navier-Stokes equation (3). The equations are solved in a frame of reference moving with the mean flow. This approach allows the application of periodic boundary conditions for the fluctuating components of the velocity field. A spectral collocation method is used for the spatial discretization and the solution is advanced in time with a fourth-order Runge-Kutta scheme. The simulations are performed on a parallel computer using a grid with 256^3 points.

As time is advanced, the coordinate system in the moving frame of reference becomes more and more skewed. Following Rogallo [23], the coordinate system is remeshed from $+45°$ to $-45°$ using the periodic structure of the dependent variables and without the need for interpolation at the chosen angles, which avoids the introduction of interpolation errors. This remeshing procedure produces aliasing errors, which are controlled by dealiasing of the affected modes before and after remeshing.

Isotropic turbulence fields are used to initialize all simulations. The values of the initial Taylor microscale Reynolds number $Re_\lambda = q\lambda/\nu = 56$ and the initial shear number $SK/\epsilon = 2$ are identical for all cases. Here $\lambda = \sqrt{5\nu q^2/\epsilon}$ is the Taylor microscale, $q = \sqrt{2K}$ is the magnitude of velocity, $\epsilon = \nu\langle\partial u_i/\partial x_k\partial u_i/\partial x_k\rangle$ is the dissipation rate, and ν is the kinematic viscosity. As time evolves, the Taylor microscale Reynolds number grows strongly and reaches values of $Re_\lambda = 120$, while the shear number quickly assumes a value of about $SK/\epsilon = 6$ in the simulations.

Mean helicity is introduced into the initial conditions following the approach described by Morinishi *et al.* [21]. The velocity vector in Fourier space is decomposed into complex-valued helical waves $\widehat{\boldsymbol{u}}(\boldsymbol{k}) = \xi_{+1}\boldsymbol{N}(\boldsymbol{k}) + \xi_{-1}\boldsymbol{N}(-\boldsymbol{k})$. Here, $\boldsymbol{N}(s\boldsymbol{k}) = \boldsymbol{e}^2(\boldsymbol{k}) - is\boldsymbol{e}^1(\boldsymbol{k})$ is the complex-valued helical wave basis [24,25] with $s = \pm 1$, ξ_{+1} and ξ_{-1} are the helical mode coefficients, and $\boldsymbol{e}^1 = \boldsymbol{k}\times\boldsymbol{a}/|\boldsymbol{k}\times\boldsymbol{a}|$ and $\boldsymbol{e}^2 = \boldsymbol{k}\times\boldsymbol{e}^1/|\boldsymbol{k}\times\boldsymbol{e}^1|$ are the basis vectors of the Craya-Herring frame [26,27]
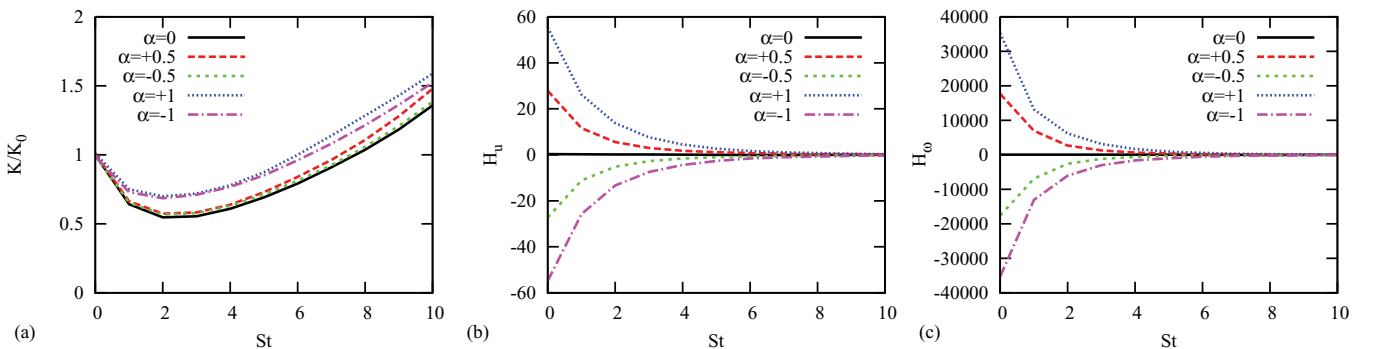

FIG. 2. (Color online) Evolution of (a) the turbulent kinetic energy K normalized by its initial value, (b) mean helicity $\langle H_u\rangle$, and (c) mean superhelicity $\langle H_\omega\rangle$ in nondimensional time St. The initial mean helicity is varied by changing α from -1 to $+1$.
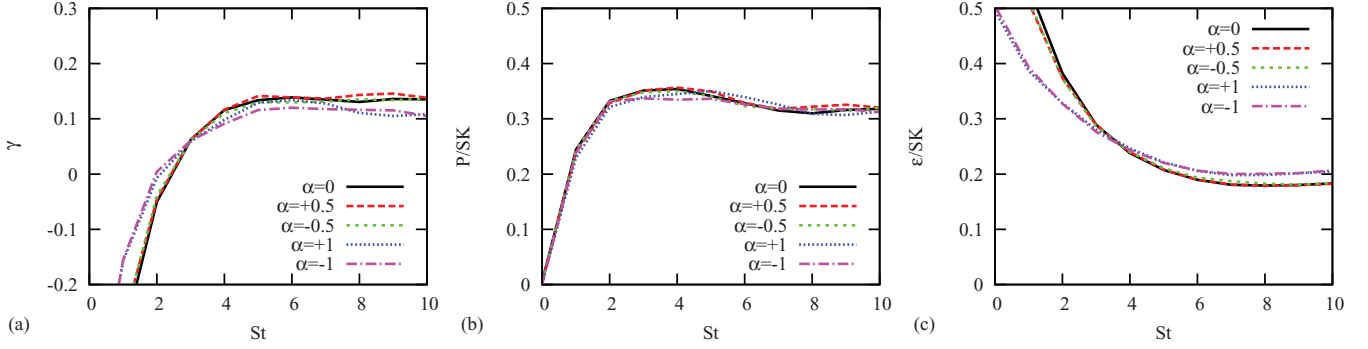
FIG. 3. (Color online) Evolution of (a) the growth rate γ, (b) normalized production $P/(SK)$, and (c) normalized dissipation $\epsilon/(SK)$. The initial mean helicity is varied by changing α from -1 to $+1$.

with $\boldsymbol{a} = (0,0,1)$ chosen for this study. Mean helicity is then introduced by changing the weights of the helical mode coefficients $\xi_{+1}^{\alpha} = \sqrt{1+\alpha}\xi_{+1}$ and $\xi_{-1}^{\alpha} = \sqrt{1-\alpha}\xi_{-1}$. Five simulations are discussed in the following with $\alpha = 0$ (no initial mean helicity), $\alpha = \pm0.5$ (moderate initial mean helicity), and $\alpha = \pm1$ (strong initial mean helicity with only one helical mode retained).

IV. RESULTS

Figure 2 shows (a) the evolution of turbulent kinetic energy K, (b) mean helicity $\langle H_u \rangle$, and (c) mean superhelicity $\langle H_\omega \rangle$ in nondimensional time St. The evolution of the turbulent kinetic energy shows an initial decay due to the isotropic initial conditions. This decay is weaker for the cases with strong initial mean helicity and it is in agreement with Kraichnan's prediction that helical motion implies a slow down of the energy transfer. Morinishi *et al.* [21] also observed a reduced decay rate for isotropic turbulence with strong initial helicity. At about nondimensional time $St = 2$, flow anisotropy develops, and turbulence production sets in. An asymptotic state with exponential growth of K is obtained at nondimensional time $St = 4$. In contrast to the exponential growth of the turbulent kinetic energy, both the mean helicity $\langle H_u \rangle$ and the mean superhelicity $\langle H_\omega \rangle$ decay as the nondimensional time St is advanced. This is expected since no production terms are present in the evolution equation for the helicity (12).
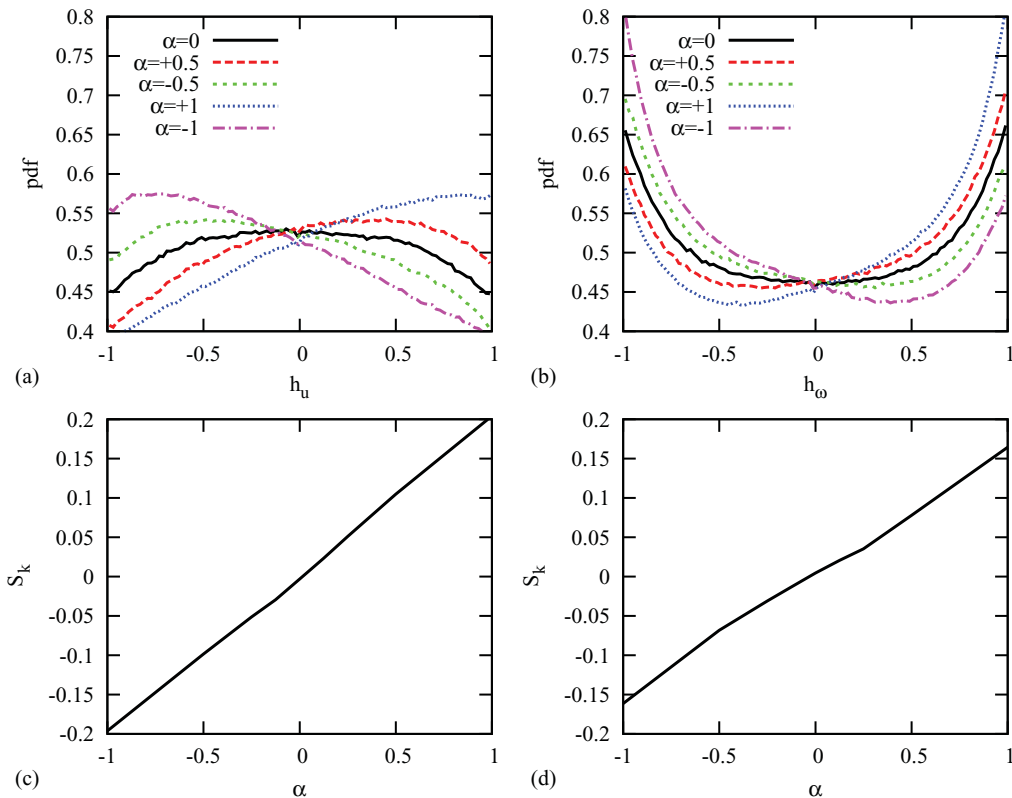

FIG. 4. (Color online) PDFs of (a) relative helicity h_u and (b) relative superhelicity h_ω. Skewness S_k of (c) relative helicity h_u and (d) relative superhelicity h_ω. The initial mean helicity is varied by changing α from -1 to $+1$.

The balance equation for the turbulent kinetic energy can be written in the nondimensional form

$$\gamma = \frac{1}{SK}\frac{dK}{dt} = \frac{P}{SK} - \frac{\epsilon}{SK}, \quad (13)$$

where γ is the nondimensional growth rate of the turbulence, $P/(SK)$ is the normalized production, and $\epsilon/(SK)$ is the normalized dissipation with $P = -S\langle u_1 u_2\rangle$. As shown in Fig. 3(a), the growth rate γ is initially negative, corresponding to the turbulence decay due to isotropic initial conditions. Again, the cases with strong initial mean helicity show initially higher growth rates, corresponding to a weaker decay of K in agreement with Morinishi *et al.* [21]. The growth rate γ eventually reaches a constant value, indicating an asymptotic state with exponential growth of the turbulent kinetic energy K.

The growth rate γ is determined by normalized production $P/(SK)$ and normalized dissipation $\epsilon/(SK)$. Figure 3(b) shows that the initial mean helicity has no impact on the turbulence production. This was expected by the analysis of the equations in Sec. II, which showed that the influence of helicity only appears in the nonlinear transfer mechanism and not in the production terms. The features of turbulence structures visualized as isovorticity surfaces (discussed later) remain unaffected by the initial value of $\langle H_u\rangle$. Figure 3(c) shows the influence of the initial mean helicity $\langle H_u\rangle$ on the normalized dissipation rate $\epsilon/(SK)$. For strong initial mean helicity $\langle H_u\rangle$, the normalized dissipation rate is initially strongly reduced, but eventually slightly increases as mean

helicity decays throughout the simulation. It appears that only the magnitude of initial mean helicity is important, and not its sign. It can be noted in this context that in the closure study by André and Lesieur [9] the helicity spectrum only appears in quadratic form in the nonlinear transfer, so that the sign does not modify the transfer. It is, however, not straightforward that this should also be true in anisotropic turbulence.

Figure 4(a) shows the probability distribution functions (PDFs) of relative helicity h_u for different initial values of the mean helicity $\langle H_u\rangle$ at nondimensional time $St = 5$. For the case without initial $\langle H_u\rangle$, an approximately symmetric PDF is found with a preference for $h_u = 0$, corresponding to a trend to two dimensionalization of the flow. With increasing initial $\langle H_u\rangle$, the PDFs are skewed corresponding to the imposed initial values of mean helicity $\langle H_u\rangle$. Figure 4(b) shows the PDFs of relative superhelicity h_ω. Again, an approximately symmetric distribution is observed for the case without initial $\langle H_u\rangle$, but a preference for $h_\omega = \pm 1$ is found. Just as for the PDFs of h_u, the PDFs of h_ω are skewed as the initial mean helicity is varied. To quantify the symmetry of the PDFs, the skewness of the relative helicities, defined by $S_k = M_3[h]/(M_2[h])^{3/2}$, where $M_p = \langle(h - \langle h\rangle)^p\rangle$ are the pth order centered moments, is shown in Figs. 4(c) and 4(d). For both helicity and superhelicity, the corresponding skewness of the PDFs increases approximately linearly with increasing initial $\langle H_u\rangle$.

In order to study the effect of initial mean helicity $\langle H_u\rangle$ on the structure of the turbulent flows, volume visualizations
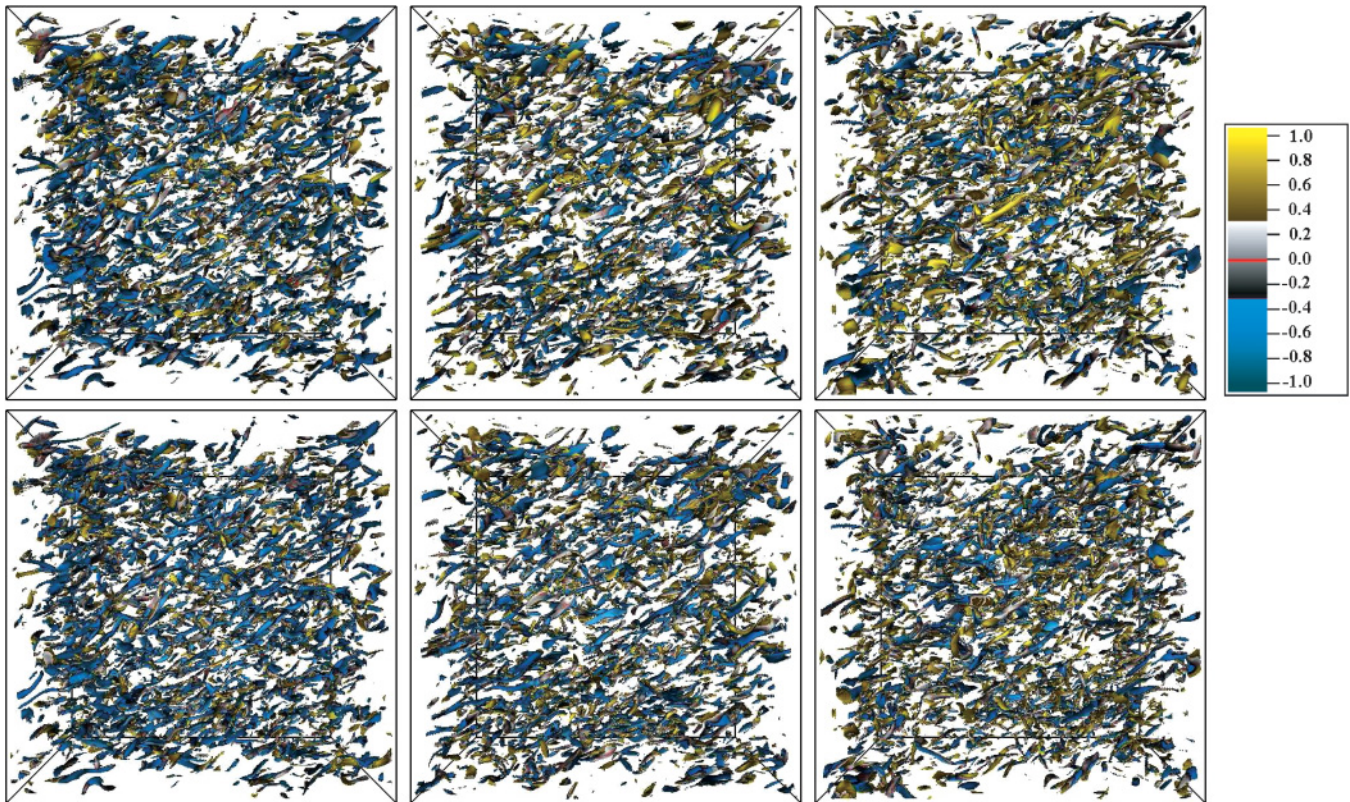

FIG. 5. (Color) Volume visualization of isovorticity colored with relative helicity h_u (top) and with relative superhelicity h_ω (bottom) for $\alpha = -1$ (left), $\alpha = 0$ (center), and $\alpha = +1$ (right). The isovalue chosen is $|\boldsymbol{\omega}| = 4\sigma_\omega$, where σ_ω is the standard deviation of $\boldsymbol{\omega}$. The view is into the negative x_3 direction and onto the plane of shear.

of the magnitude of fluctuating vorticity are considered. For details on volume visualization see Ref. [28]. Figure 5 shows vortical structures for cases with $\alpha = -1$ (left), $\alpha = 0$ (center), and $\alpha = +1$ (right) at nondimensional time $St = 5$. The vortical structures are inclined in the vertical direction relative to the downstream direction due to shear. The features of the vortical structures remain unchanged as the initial helicity $\langle H_u \rangle$ is varied. The structures are colored with the values of the relative helicity h_u (top) and relative superhelicity h_ω (bottom). For the case with $\alpha = -1$ (left), the initial mean helicity $\langle H_u \rangle$ is negative and a predominance of negative values of both h_u and h_ω is observed in the figure. For $\alpha = 0$ (center), the initial $\langle H_u \rangle$ is close to zero and positive and negative values of h_u and h_ω are in balance. For $\alpha = +1$ (right), the initial $\langle H_u \rangle$ is positive and a predominance of positive values of h_u and h_ω is found. For a given flow structure, it is likely that the same color for h_u and h_ω is observed for the same initial mean helicity case. Therefore, the signs of relative helicity and relative superhelicity are strongly correlated.

The scale-dependent helicity, proposed in Ref. [18], is defined as $H_{u^j} = \mathbf{u}^j \cdot \boldsymbol{\omega}^j$, where $\mathbf{u}^j$ and $\boldsymbol{\omega}^j$ are velocity and

vorticity at scale 2^{-j}, respectively. For $j \neq 0$, H_{u^j} preserves Galilean invariance, though helicity H_u itself does not. The scale contributions of velocity $\mathbf{u}^j$ (and similarly for vorticity and its curl) are obtained by decomposing each component of $\mathbf{u}$, given at resolution $N = 2^{3J}$ with $J = 8$, into an orthogonal wavelet series using Coiflet 12 wavelets

$$\mathbf{u}(\mathbf{x}) = \sum_\lambda \widetilde{\mathbf{u}}_\lambda \psi_\lambda(\mathbf{x}), \tag{14}$$

where the multi-index $\lambda = (j, \mathbf{i}, \mu)$ denotes scale j (with $0 \leqslant j \leqslant J - 1$), spatial position $\mathbf{i}$ (with 2^{3j} values for each j and μ), and seven spatial directions $\mu = 1, \ldots, 7$ of each wavelet ψ_λ [29,30]. Orthogonality implies that the wavelet coefficients are given by $\widetilde{\mathbf{u}}_\lambda = \langle \mathbf{u}, \psi_\lambda \rangle$, where $\langle \cdot, \cdot \rangle$ denotes the L^2-inner product. The coefficients measure fluctuations of $\mathbf{u}$ at scale 2^{-j} and around position $\mathbf{i}/2^j$ for each of the seven possible directions. Fixing j and summing only over $\mathbf{i}$ and μ in Eq. (14) the contribution of $\mathbf{u}$ at scale j is obtained and by construction we have $\mathbf{u} = \sum_j \mathbf{u}_j$.

The scale-dependent relative helicity is defined by $h_{u^j} = H_{u^j}/(|\mathbf{u}^j||\boldsymbol{\omega}^j|)$. Analogously, the scale-dependent
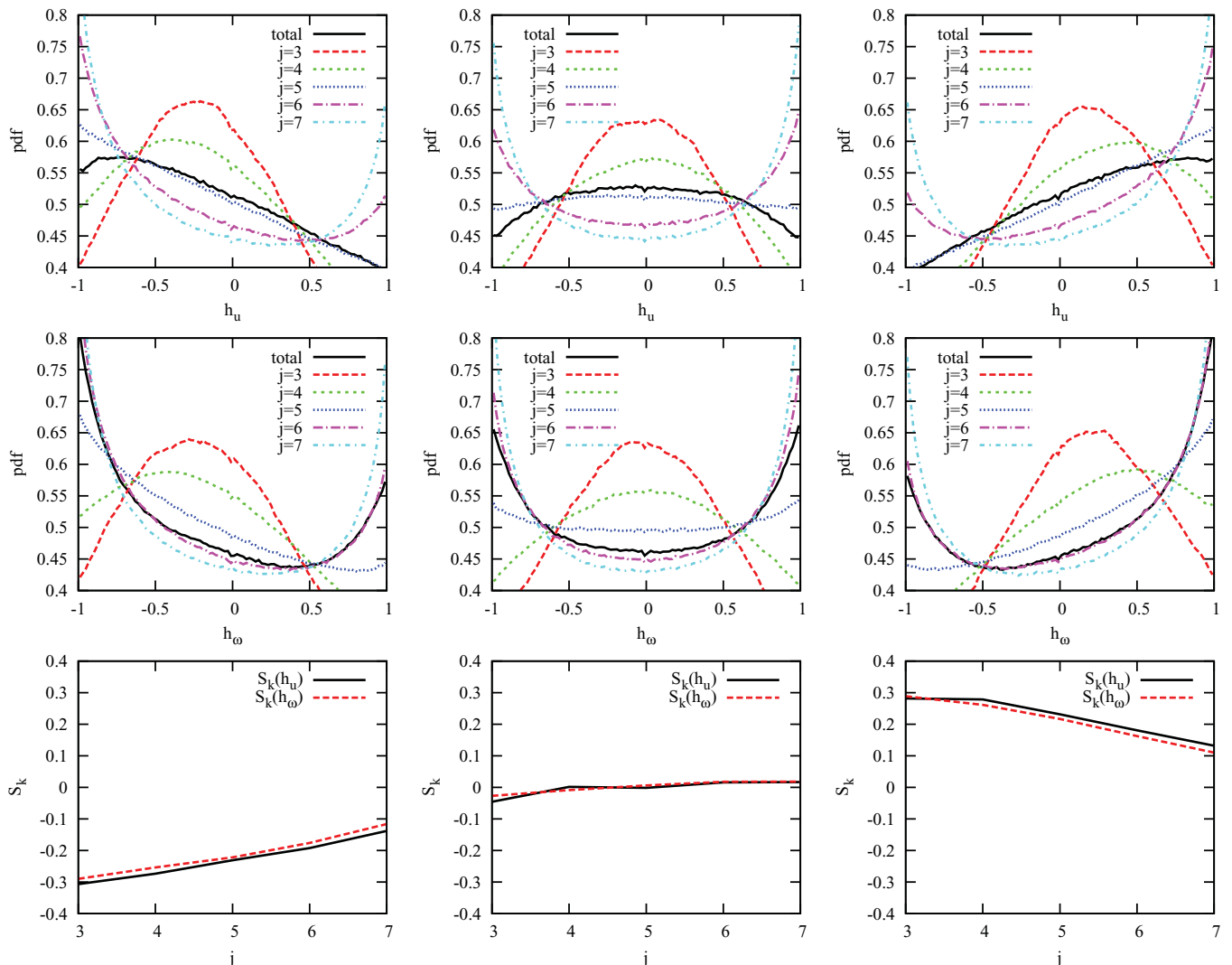

FIG. 6. (Color online) Scale-dependent helicity distribution h_{u^j} (top), superhelicity distribution h_{ω^j} (center), and skewness of helicity and superhelicity (bottom) for $\alpha = -1$ (left), $\alpha = 0$ (center), and $\alpha = +1$ (right).

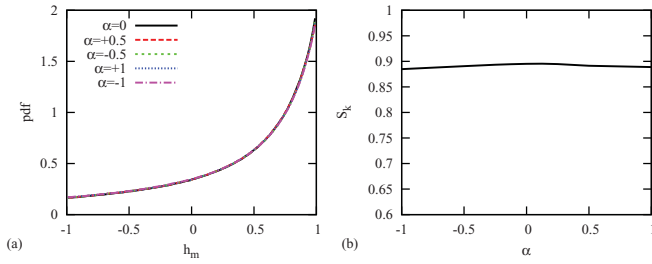FIG. 7. (Color online) (a) PDF and (b) corresponding skewness of the product $\boldsymbol{u} \cdot \boldsymbol{\nabla} \times \boldsymbol{\nabla} \times \boldsymbol{u}/(|\boldsymbol{u}||\boldsymbol{\nabla} \times \boldsymbol{\nabla} \times \boldsymbol{u}|)$. The initial mean helicity is varied by changing α from -1 to $+1$.

superhelicity $H_{\omega^j} = \boldsymbol{\omega}^j \cdot (\boldsymbol{\nabla} \times \boldsymbol{\omega})^j$ and the corresponding relative quantity h_{ω^j} can be obtained. The skewness of the scale dependent helicities is defined accordingly, replacing the total quantities by their scale-dependent counterparts. The above scale-dependent quantities will help to gain a better understanding of geometrical statistics at different scales of motion.

PDFs of scale-dependent relative helicity h_{u^j} (top), relative superhelicity h_{ω^j} (center), and the corresponding skewness (bottom) are presented in Fig. 6 for cases with strong negative initial mean helicity ($\alpha = -1$, left), no significant initial mean helicity ($\alpha = 0$, center), and strong positive initial mean helicity ($\alpha = +1$, right). For the case without initial $\langle H_u \rangle$, the larger scales of motion with $j = 3, 4$, and 5 show a preference for $h_u = 0$, corresponding to a trend to two dimensionalization of the flow. The smaller scales with $j = 6$ and 7 have maxima at $h_{u^j} = \pm 1$, corresponding to a trend to helical motion at small scales. For the cases with strong initial $\langle H_u \rangle$, a similar result is obtained, however the PDFs are skewed. This effect is more pronounced at larger scales, indicating a stronger effect of initial mean helicity on large scales than on small scales of the turbulent motion. Similar results are obtained for PDFs of relative superhelicity h_ω [see Fig. 6 (center)]. For isotropic helical turbulence, Kraichnan [8] predicted that helicity has a stronger influence on large scales than on small scales under the assumption of a local helicity cascade.

For isotropic turbulence, Sanada [19] discussed the balance equation for mean helicity (5) and conjectured that the dissipation of mean helicity is determined by mean superhelicity. As neither mean helicity nor mean superhelicity are positive definite, it is required that both quantities assume the same sign

for this to be true. Thus this sign correlation strongly impacts the dynamics of helicity. Statistically, this correlation should hold if a local and linear helicity cascade exists. By linear we mean here that the flux of helicity to the small scales is linearly dependent on the helicity dissipation in a statistically stationary case, equivalent to the case of a passive scalar. The linearity of the helicity cascade was illustrated in forced isotropic helical turbulence in the work by Borue and Orszag [6]. If the flux of helicity in homogeneous shear flow is linear, then the mean superhelicity is expected to have the same sign as the mean helicity of the flow. This does however not imply that in a flow field this holds locally and instantaneously. This will now be investigated.

As shown in Fig. 7(a), the PDF of the cosine of the angle between velocity $\boldsymbol{u}$ and the negative Laplacian of velocity $-\nabla^2 \boldsymbol{u} = \boldsymbol{\nabla} \times \boldsymbol{\nabla} \times \boldsymbol{u}$, a quantity related to velocity dissipation, indicates a much larger probability that the two vectors are aligned. The initial value of $\langle H_u \rangle$ has no impact on these PDFs and the skewness, shown in Fig. 7(b), remains constant. We anticipate that, even in the case of a divergence-free Gaussian random field, the cosine of the angle between velocity and its Laplacian shows a larger probability that the two vectors are aligned. This suggests that the alignment is at least partially a kinematic property of the Laplace operator.

Note also that the mean value is positive $-\langle \boldsymbol{u} \cdot \nabla^2 \boldsymbol{u} \rangle = \langle \boldsymbol{\omega} \cdot \boldsymbol{\omega} \rangle > 0$. This implies the tendency that $H_u = \boldsymbol{u} \cdot \boldsymbol{\omega}$ and $H_\omega = -\nabla^2 \boldsymbol{u} \cdot \boldsymbol{\omega}$ have the same sign [19], a tendency which also holds for the relative helicities [20]. This again seems to corroborate the picture of a linear helicity transfer in which the superhelicity is linearly proportional to the helicity.

To verify this conjecture for the homogeneous turbulent shear flow considered here, the joint PDFs of relative helicity h_u with relative superhelicity h_ω are shown in Fig. 8. In the case $\alpha = -1$ (left) we obtain a pronounced peak at $h_u = -1$ and $h_\omega = -1$, while the peak at $h_u = 1$ and $h_\omega = 1$ is weak. In the case $\alpha = 0$ (center), the two peaks at $h_u = -1$ and $h_\omega = -1$ as well as $h_u = 1$ and $h_\omega = 1$ are of the same strength. In the case $\alpha = 1$ (right), a pronounced peak at $h_u = 1$ and $h_\omega = 1$ is observed, while the peak at $h_u = -1$ and $h_\omega = -1$ is weakened.

In summary, a strong correlation of the signs of the two helicities is observed for all cases, supporting the conjecture that superhelicity diminishes helicity. In addition, the joint PDF is approximately symmetric to the origin for the case
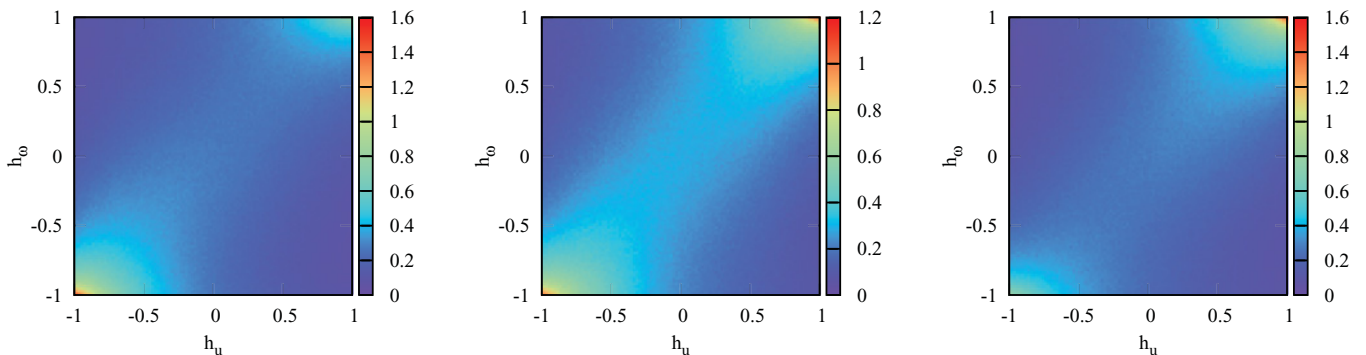

FIG. 8. (Color online) Joint PDF of helicity h_u and superhelicity h_ω for $\alpha = -1$ (left), $\alpha = 0$ (center), and $\alpha = +1$ (right).

without initial mean helicity and this symmetry is broken for cases with initial mean helicity.

V. CONCLUSIONS

To summarize, helical properties of homogeneous turbulent shear flow were investigated. Initial mean helicity is imposed on the flow following an approach developed by Morinishi *et al*. [21]. Initial mean helicity weakens the initial decay of turbulent kinetic energy in the simulations before anisotropic shear production sets in. These findings are in agreement with Kraichnan's prediction that helical motion implies a slow down of the energy transfer. The eventual evolution of the energy remains relatively unaffected by initial mean helicity, since helicity does not directly influence the production of turbulent kinetic energy. For the PDFs of relative helicity h_u, a maximum at $h_u = 0$ was observed for the case without initial mean helicity. For cases with initial mean helicity, the PDFs of h_u are increasingly skewed depending on the initial level of mean helicity. The PDFs of relative superhelicity, however, always exhibit maxima for $h_\omega \pm 1$ with a skewness also depending on the initial mean helicity.

Scale-dependent PDFs of helicity show that large scales tend to have a maximum at $h_{u^j} = 0$, which provides evidence for two dimensionalization of the flows at large scales, while small scales tend to show a maximum at $h_{u^j} = \pm 1$, corresponding to helical motion at small scales. The PDFs are skewed at all scales in the presence of initial mean helicity, and this effect decreases at smaller scales of the turbulent motion.

Sanada [19] conjectured that the dissipation of mean helicity is determined by mean superhelicity. Joint PDFs of relative helicity and relative superhelicity show indeed a high probability that h_u and h_ω have the same sign even locally. In conclusion, superhelicity dissipates helicity for anisotropic shear-driven turbulence.

[1] H. K. Moffatt and A. Tsinober, Annu. Rev. Fluid Mech. **24**, 281 (1992).

[2] A. Pouquet, M. Lesieur, and J. Leorat, J. Fluid Mech. **77**, 321 (1976).

[3] R. Betchov, Phys. Fluids **4**, 925 (1961).

[4] J.-J. Moreau, C. R. Acad. Sci. Paris **252**, 2810 (1961).

[5] H. K. Moffatt, J. Fluid Mech. **35**, 117 (1969).

[6] V. Borue and S. A. Orszag Phys. Rev. E **55**, 7005 (1997).

[7] Q. Chen, S. Chen, and G. L. Eyink, Phys. Fluids **15**, 361 (2003).

[8] R. H. Kraichnan, J. Fluid Mech. **59**, 745 (1973).

[9] J. C. André and M. Lesieur, J. Fluid Mech. **81**, 187 (1977).

[10] E. Levich and A. Tsinober, Phys. Lett. A **93**, 293 (1983).

[11] R. Pelz, V. Yakhot, S. Orszag, L. Shtilman, and E. Levich, Phys. Rev. Lett. **54**, 2505 (1985).

[12] R. H. Kraichnan and R. Panda, Phys. Fluids **31**, 2395 (1988).

[13] W. Polifke and L. Shtilman, Phys. Fluids A **1**, 2025 (1989).

[14] P. D. Mininni and A. Pouquet, Phys. Fluids **22**, 035105 (2010).

[15] P. D. Mininni and A. Pouquet, Phys. Fluids **22**, 035106 (2010).

[16] R. Benzi, L. Biferale, R. M. Kerr, and E. Trovatore, Phys. Rev. E **53**, 3541 (1996).

[17] L. Biferale, D. Pierotti, and F. Toschi. Phys. Rev. E **57**, R2515 (1998).

[18] K. Yoshimatsu, N. Okamoto, K. Schneider, Y. Kaneda, and M. Farge, Phys. Rev. E **79**, 026303 (2009).

[19] T. Sanada, Phys. Rev. Lett. **70**, 3035 (1993).

[20] B. Galanti and A. Tsinober, Phys. Lett. A **352**, 141 (2006).

[21] Y. Morinishi, K. Nakabayashi, and S. Ren, JSME International Journal Series B **44**, 410 (2001).

[22] C. Cambon, D. Jeandel, and J. Mathieu, J. Fluid Mech. **104**, 247 (1981).

[23] R. S. Rogallo, NASA Report No. TM 81315, 1981.

[24] C. Cambon and L. Jacquin, J. Fluid Mech. **202**, 295 (1989).

[25] F. Waleffe, Phys. Fluids A **4**, 350 (1992).

[26] A. Craya, Contribution à l'analyse de la turbulence associée à des vitesses moyennes. P. S. T. Ministère de l'Air, Paris, 345, 1958.

[27] J. R. Herring, Phys. Fluids **17**, 859 (1974).

[28] J. Clyne, P. Mininni, A. Norton, and M. Rast, New J. Phys. **9**, 301 (2007).

[29] M. Farge. Annu. Rev. Fluid Mech. **24**, 395 (1992).

[30] K. Schneider and O. Vasilyev, Annu. Rev. Fluid Mech. **42**, 473 (2010).